Computer Simulation of High Pressure Plasmas based on PHOENICS

J D Yan, J L Zhang, V K Liau, C M Dixon and M T C Fang

Department of Electrical Engineering and Electronics
University of Liverpool, Liverpool L69 3GJ, UK

Abstract

Computer simulation of high-pressure plasmas requires, in most cases, the solutions of Navier-Stokes Equations modified to include Ohmic input, Lorentz force and radiation transport. Relevant Maxwell's equations are included for the calculation of electromagnetic fields. In some applications, the ablation of inner surface of the plasma-containing vessel and the subsequent entrainment of the wall vapour change the device characteristics. The consideration of the effects of ablation necessitates the introduction of a vapour concentration equation. Electrodeless plasmas maintained by microwave the plasma are often not in local thermal equilibrium. For such a plasma at atmospheric pressure a two-temperature model is needed to describe the plasma behaviour. An auto-expansion circuit breaker, a rotary arc device and a microwave generated plasma jet are used to illustrate the power of PC based PHOENICS. Computer simulated results are in agreement with available experimental results.

Content List

1. Introduction

A large number of industrial devices utilises plasma as an intense heat source. Such devices include arc furnaces, torches, heaters, welding machines, high power switchgear etc. These devices are used for material melting and forming, cutting, heating, waste destruction, surface modification, light sources, and, more recently, for growing carbon nanotubes. The power level of these devices ranges from megawatts to tens of watts. The plasma is usually maintained by a passage of a current or by a microwave source. The plasma is often in motion driven by a pressure gradient (self-generated or externally imposed) and/or by a Lorentz force due to the arcing current interacting with an externally imposed magnetic field or with the magnetic field generated by the current itself.

Because of the plasma is at atmospheric pressure or above and at high power level, the constituent species (electrons, ions, atoms and molecules) of the plasma attain a single temperature. Such plasma is commonly known as thermal plasma. The thermodynamic state (local thermal equilibrium) of the plasma can therefore be described by two thermodynamic variables. Within such a plasma system the plasma temperature often reaches 20,000K to 30,000K on the device axis and decays rapidly to ambient temperature. In some devices, the plasma is accelerated in a space of 10cm to a velocity of a few thousand meters. The flow is often turbulent. At such high temperature, radiation transport becomes an extremely important energy transfer mechanism. In a number of high power devices the arc strongly interacts with its surroundings resulting in electrode melting and the ablation of the inner surface of the containing vessel. As a result, the composition of the arc can be substantially altered, which may change the operational characteristics of the device and its life.

For microwave generated plasmas, the power input often concentrates in a very small volume. The rate of power transfer from electrons in this volume to the heavy particles is not sufficiently fast to ensure that the plasma is in local thermal equilibrium. The adoption of a two-temperature model is therefore necessary.

In general, engineering systems using high pressure plasma as the main system component are expensive to develop and difficult to scale. Computer aided simulation and design tools are therefore extremely useful. The success of such tools depends on a sufficiently accurate description of the dominant physical processes and on the robust algorithms which can solve a set of highly non-linear partial differential equations describing electromagnetic fields, temperature and velocity field with moving boundaries. Computational costs in recent years have been drastically reduced and PC based computer simulation has become a useful tool in design offices.

PHOENICS has been proven to be a powerful, versatile simulation tool in dealing with engineering systems employing high pressure arcs. In this paper, two high power circuit breakers and a microwave generated plasma jet are used to demonstrate the potential of PHOENICS as a simulation tool. Whenever possible, simulated results are compared with experiments.

2. Simulation of the Operation of High Power Circuit Breakers

Modern circuit breakers are required to interrupt a fault of up to a peak current of 80kA and with a system voltage 400kV and above. To reduce the manufacturing cost, arc energy in the high current phase has to be utilised to create the flow conditions at current zero for the extinction of the arc at an AC current zero. Even for circuit breakers at medium power and voltage levels, environmental restrictions and cost considerations require the circuit breaker as compact as possible. Thus, the effects of changing a single design parameter are difficult to predict even for experienced designers. Computer simulation has become a necessary part of a design process. The PC based PHOENICS is an ideal platform for the development of CAD tools for these breakers.

As mentioned previously, the arc in a circuit breaker can be treated as a single fluid, which can be described by Navier Stokes equations modified to take into account the Lorentz force, Ohmic heating and radiation transport. Additional equations, species concentration equations, need to be introduced to take into account of inner surface ablation of the arc containing vessel and the vaporisation of electrode. Relevant Maxwell's equations provide the required electromagnetic fields. Thus, the governing equations for axisymmetrical systems are given by

$$\frac{\partial(\rho\phi)}{\partial t} + \nabla \bullet (\rho\phi\vec{V}) - \nabla \bullet (\Gamma_\phi \nabla\phi) = S_\phi \qquad (1)$$

where ρ and $\vec{V}$ are respectively the density and mass-averaged velocity of the mixture. The dependent variable ϕ, diffusion coefficient Γ_ϕ and source term S_ϕ are listed in Table 1. The subscript *l* denotes the laminar part of the diffusion coefficient and *t* the turbulent part.

Table 1

Equation	ϕ	Γ	S_ϕ
mass of mixture	1	0	0
θ-momentum (azimuthal)	u	$\mu_l + \mu_t$	$-\frac{\rho v u}{r} - \frac{(\mu_l+\mu_t)u}{r^2} - \frac{u}{r}\frac{\partial}{\partial r}(\mu_l+\mu_t) + (J\times B)_\theta$
z-momentum	w	$\mu_l + \mu_t$	$-\partial P/\partial z + (J\times B)_z$ + viscous terms
r-momentum	v	$\mu_l + \mu_t$	$-\partial P/\partial r - (J\times B)_r$ + viscous terms
enthalpy	h	$(k_l+k_t)/c_p$	$\sigma E^2 - q + dP/dt$ + viscous dissipation
PTFE/electrode vapour mass concentration	c_m	$\rho(D_l+D_t)$	0

The radiation transport can be accounted for by introducing net emission coefficient and by introducing a radiation reabsorption layer as given in [1]. The description of a electromagnetic field is device dependent, which is therefore given in the appropriate sections.

Prandtl mixing length model (PHOENICS default) is used to calculate the turbulence enhanced momentum and energy transfer in the plasma region when there is no swirling flow. For a rotary arc circuit breaker, we assume isotropy for turbulent viscosity in the r-z and r-θ plane. Isotropy sets $\mu_t = \mu_{rz} = \mu_{r\theta}$, and μ_t is defined as [2]

$$\mu_t = \rho l_m^2 \left\{ \left(\frac{\partial w}{\partial r}\right)^2 + \left[r\frac{\partial}{\partial r}\left(\frac{u}{r}\right)\right]^2 \right\}^{1/2} \qquad (2)$$

The turbulence length scale in both cases is taken as a fraction (0.1) of the arc's thermal radius [1]. A slight modification to the source term for the radial momentum conservation equation is also needed with a rotary arc circuit breaker.

2.1 Auto-expansion Circuit Breaker

2.1.1 Computation of electric and magnetic fields

These breakers are used for ultra-high voltages. Figure 1 shows a 245kV auto-expansion breaker, where the moving contact travels at a given speed. The breaker is subjected to an arcing current as specified in Figure 2.

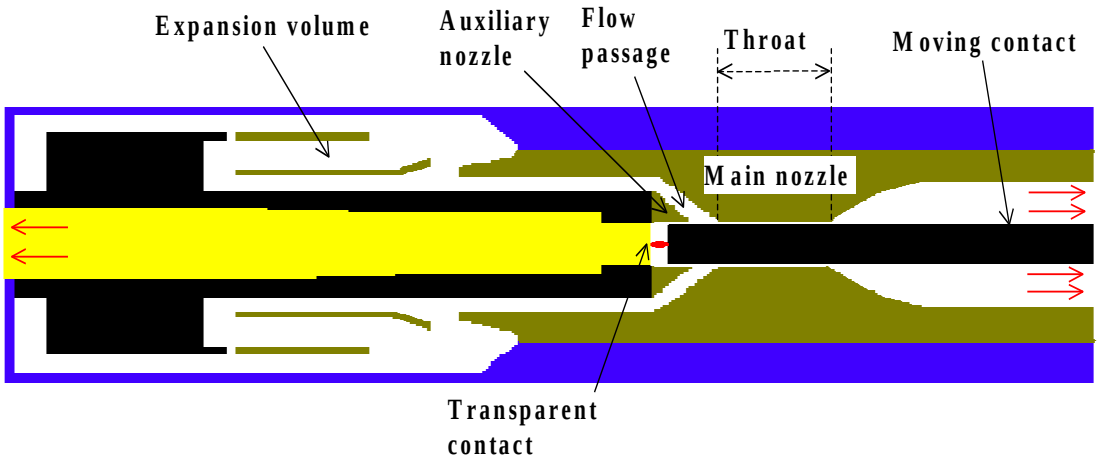

Figure 1 Schematic diagram of the 245kV auto-expansion circuit breaker.

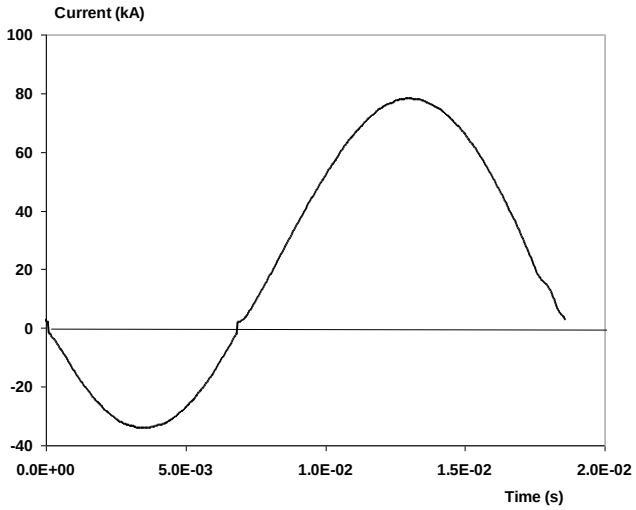

Figure 2 Arcing current specified for the 245kV auto-expansion circuit breaker.

AC arcs are low frequency plasma and the solution of the electric and magnetic fields can be separated. The current density, $\vec{j}^{\omega}$, depends on the electric field through Ohm's law

$$\vec{j} = \sigma \vec{E} \tag{3}$$

The electric field, $\vec{E}^{\omega}$, can be expressed as the negative gradient of a scalar potential, V, which can be calculated from the equation of charge conservation

$$\nabla \cdot (\sigma \nabla V) = 0 \tag{4}$$

where σ is the electrical conductivity. The computation domain for V is much larger than that for the fluid as electricl force is of long range in nature. Since the arc is axisymmetric, the magnetic flux density is given by

$$\frac{1}{r}\frac{\partial}{\partial r}(rB_\theta) = \mu_0 j_z \tag{5}$$

where $\mu_0 = 4\pi \times 10^{-7}$ H/m is the permeability of free space and j_z is the axial current density component.

2.1.2 Material properties and boundary conditions

The closure of the equations needs the information on the equation of state and the dependence of transport properties such as electric conductivity, viscosity, thermal conductivity and the diffusivity of PTFE/electrode vapour in the gas mixture as functions of pressure, enthalpy and the PTFE/electrode vapour mass concentration. For the gas mixture of SF_6-PTFE vapour, they have been tabulated in [3]. The boundary conditions for velocity, enthalpy, and electrostatic potential are given in [1].

2.1.3 Inner wall ablation

A large proportion of radiation from the high temperature arc escapes from the arc [1]. The intense radiation flux incident upon the inner face of arc containing vessel causes radiation induced ablation. The material of the surface is usually PTFE, the ablation rate of which is related to the radiation flux through

$$F(1-\alpha)Q = \dot{m}h_a \tag{6}$$

where Q is the total radiation flux per unit length and $\dot{m}$ the rate of ablation per unit length. h_a is the total energy required to break up the chain of PTFE molecules (depolymerisation) and to raise a unit mass of ablated PTFE vapour from room temperature to 3,400K[1]. The empirical factor, F, is set to 0.9 in the present work. α is a re-absorption factor, which is related to the instantaneous arcing current and nozzle cross section [1].

2.1.4 Grid system, time step, input of material properties and electric potential solver

A body-fitted grid system is used in the computation to model the complex geometry of the arcing chamber. There are altogether 74 (radial direction) by 122 (axial direction) cells in the flow field computation domain (Figure 1). To resolve the steep gradient of arc parameters, 45 cells are used in the first 10mm in the radial direction. The cell size in the flow passage, which connects the expansion volume and the main nozzle (Figure 1), is about 1mm ×1mm. The influence of the cell size in the arc region is checked by doubling the number of cells in both directions. Results for a steady state case with arcing current of 45kA in the same main nozzle show that the maximum difference in arc temperature is less than 3%. The difference in arc voltage is negligible.

The arc is initiated at time zero with a current of 2kA across a gap of 8mm between the transparent and solid contacts by introducing a conducting plasma column across the gap. The solid contact, which is labelled as the 'Moving contact' in Figure 1, starts to move with a speed of 7.14m/s at an instant of 1.12ms after arc initiation. The arcing duration is 18.6ms with a second peak current of 78kA at 13ms (Figure 2). The total time is divided into two regions: the first 20 time-steps is used for a period of 2μs over which the arc parameters experience rapid change and 930 time-steps over the remaining time. The time step is distributed uniformly in both regions.

The filling pressure of SF_6 is 0.69MPa absolute. All the thermodynamic and transport properties including the diffusivity of PTFE/electrode vapour in the gas mixture have been tabulated and coded into GROUND file by user-defined subroutines.

Solution of the charge conservation equation (4) in a transient CFD problem can be achieved by solving the PHOENICS equation for TEM1 with the transient, convective and source terms deactivated. The only material property needed is the electrical conductivity. Neumann boundary condition is applied to the boundaries of the electric potential domain except that at the ends of the two electrodes where the potential is fixed to given values. At the end of each sweep of interation, the electric current under the above fixed potential conditions is calculted and the potential field is linearly scaled according to the specified current. The electric and magnetic fields are then calculated by a user-defined subroutine. Results show that the FIX POTENTIAL approach works satisfactorily in simulation of auto-expansion circuit breakerarcs.

2.1.5 Simulation results

The operation of a 245kV, 78kA auto-expansion breaker (Figure 1) with the measured speed of contact separation is simulated for the given current wave form. The arc rooting at the hollow electrode is simulated by a transparent (to the flow) electrode, which collects the arc current [4]. This is a reasonable approximation at currents above a few kAs as the arc would block the hollow cathode.

The major advantage of computer simulation is the visualisation of the detailed flow, electric, and magnetic fields. Typical results of the whole operation cycle are given in Figure 3 for the PTFE mass concentration, Figure 4 for the temperature fields, in Figure 5 for the electric fields, and Figure 6 for the pressure distribution.

The flow conditions at current zero are critically dependent upon the composition, temperature, and pressure distribution within the auto-expansion volume. A sequence of pictures (Figure 7) shows the mixing process of the cold SF_6 originally in the volume with the oncoming hot mixture of SF_6/PTFE vapour. When the current approaches the second current zero the gas between the two contact is more or less pure SF_6, thus maintaining the superior arc quenching ability of SF_6.

The calculated arc voltage and pressure rise in the expansion volume are compared with the short circuit test results in Figure 8, which gave satisfactory agreement.

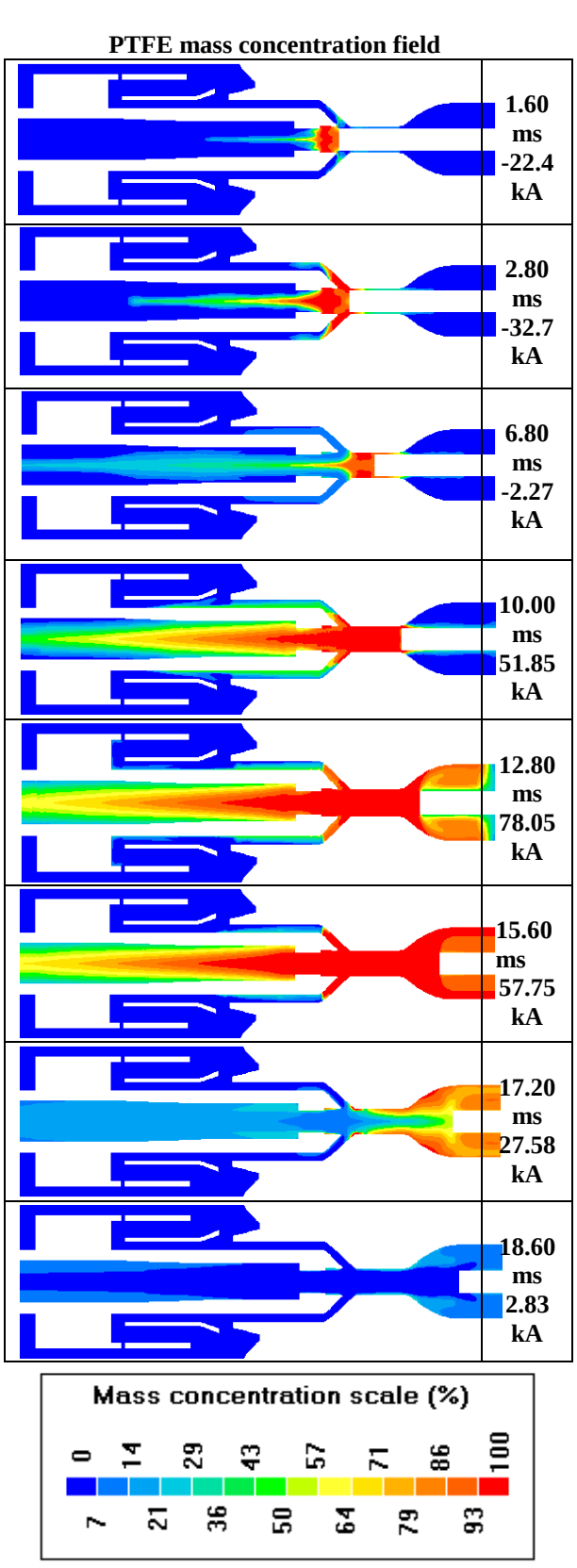

Figure 3 Typical results of the PTFE mass concentration.

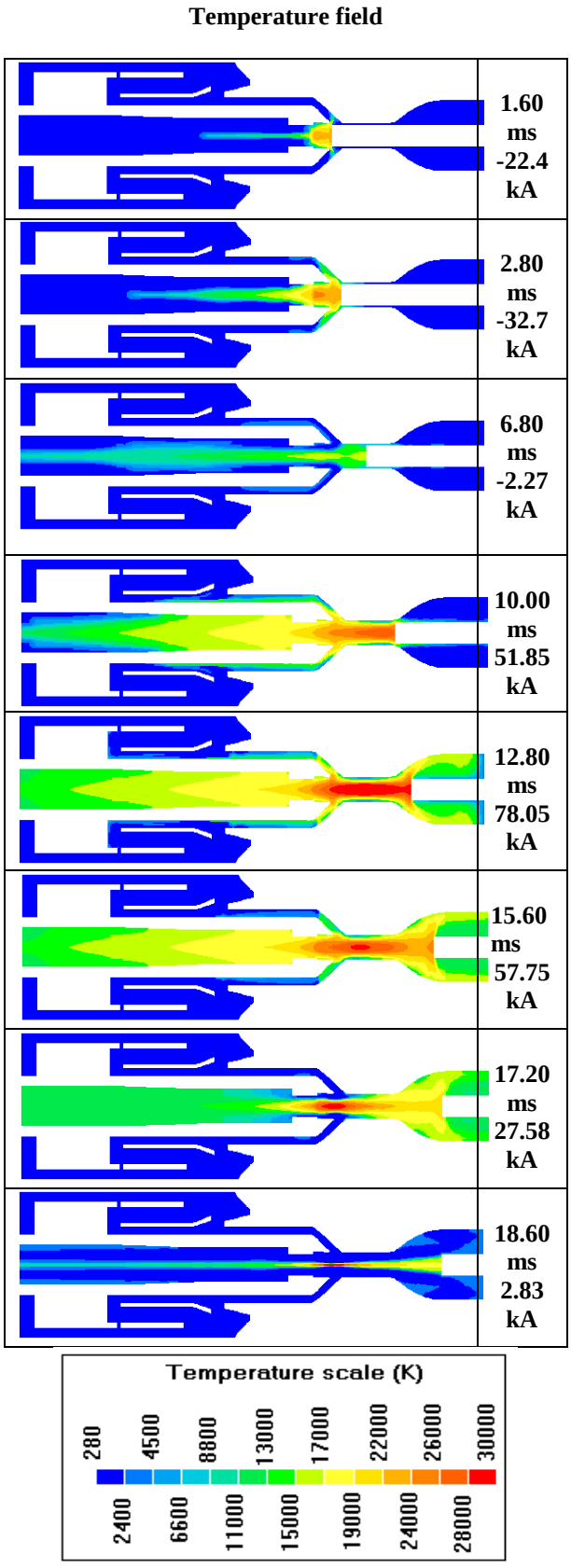

Figure 4 Typical results of the temperature.

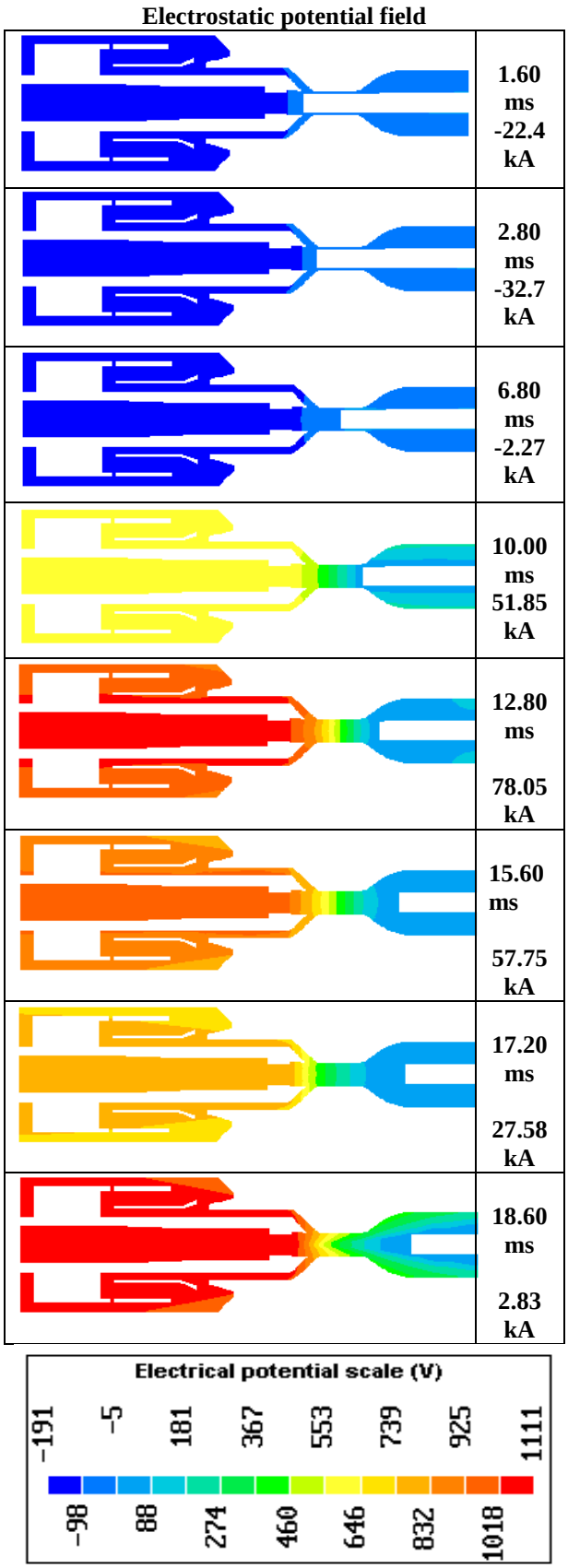

Figure 5 Typical results of the electrostatic potential.

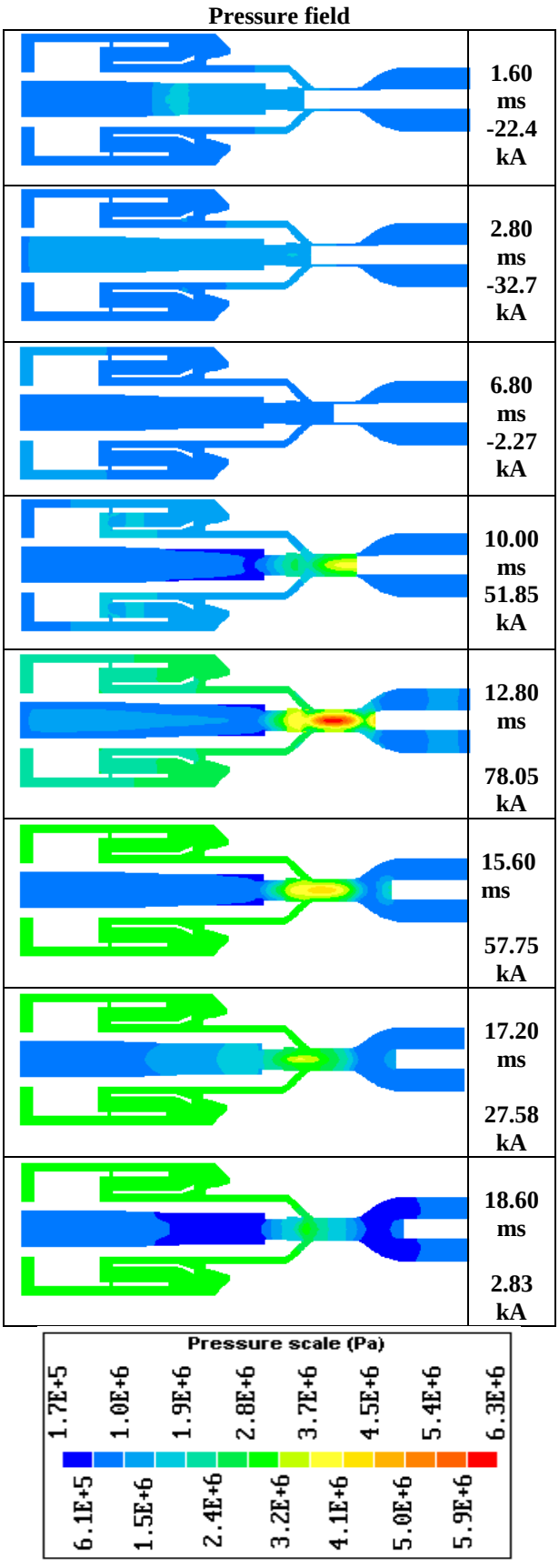

Figure 6 Typical results of the pressure.

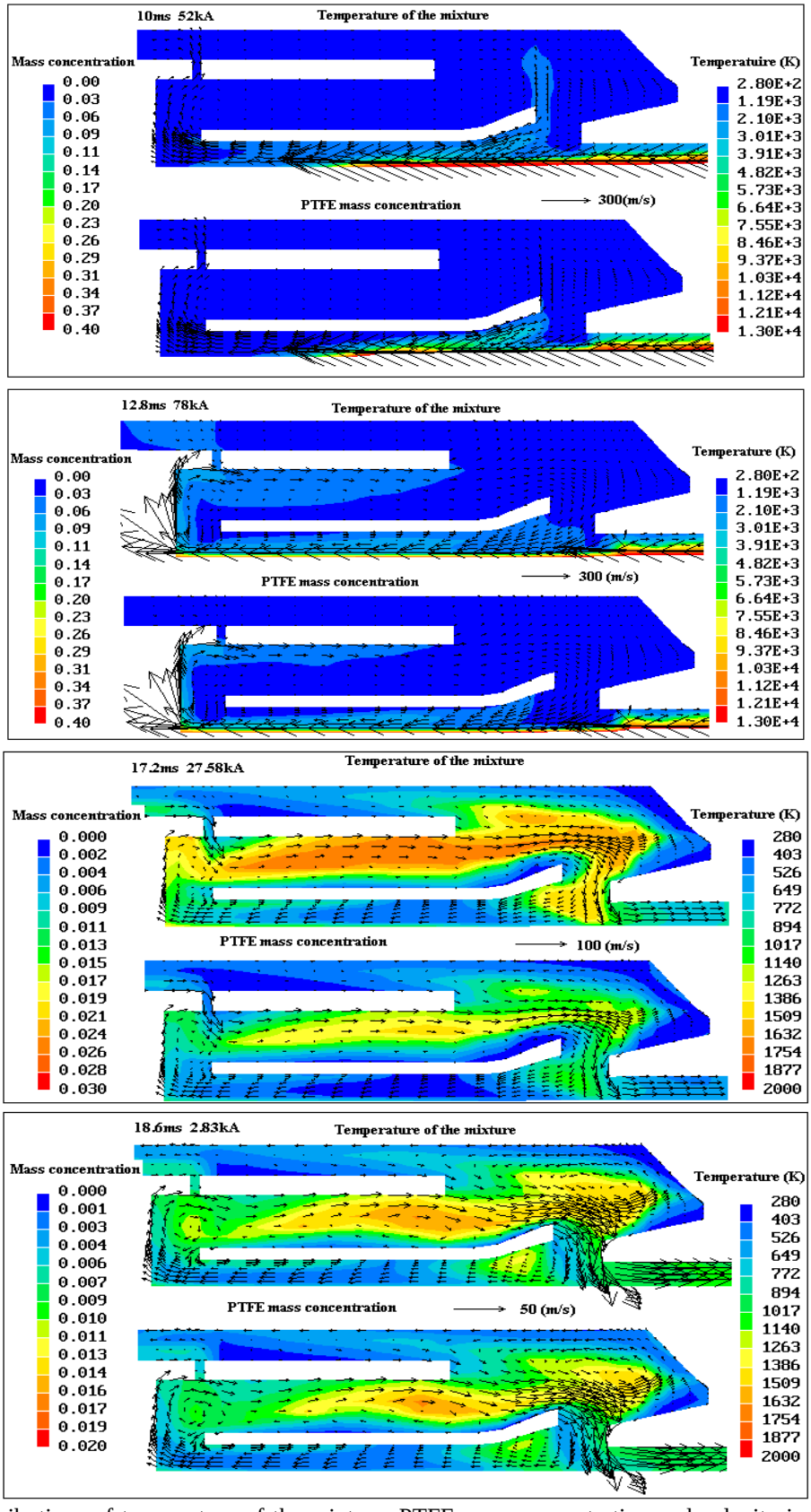

Figure 7 Distributions of temperature of the mixture, PTFE mass concentration and velocity in the expansion volume.

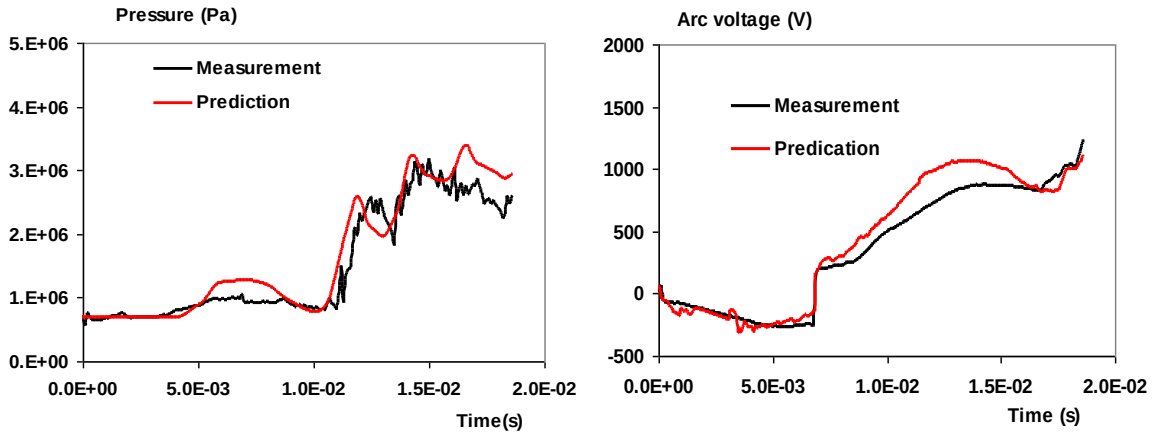

Figure 8 Predicted and measured pressure rise in the expansion volume and arc voltage.

2.2 A Rotary Arc Circuit Breaker

2.2.1 *The governing equations*

At distribution voltage level, an external magnetic field is introduced to reduce the size of the breaker and the energy requirement of the operation mechanism. As in the auto-expansion circuit breaker, arc energy during the high current phase is utilised to create the right pressure for arc extinction. The external magnetic field is to ensure arc extinction at small peak currents.

The magnetic field for the breaker (Figure 9) is produced by the external coil. The current in the coil is usually equal to the arcing current. Because of the metallic parts within the interrupter, the induced eddy currents in these parts can substantially influence the magnetic fields. In addition, the presence of the arc will in turn change the magnetic field. Thus, the magnetic field is closely coupled to the arc and the electric field through power input. We therefore need to simultaneously solve the magnetic and electric fields, temperature, pressure and the velocity fields. The method of computation of the magnetic field differs from that for auto-expansion circuit breaker. For the field produced by the external coil, we derive the magnetic field from the vector potential, A, which is given for axisymmetrical case by

$$\nabla^2 \vec{A} = \begin{cases} -\mu_0 \vec{j}_s, \text{ in the coil} \\ \mu\sigma \dfrac{\partial}{\partial t}(\vec{A}) \text{ in other conducting parts} \\ 0 \text{ in non-conducting parts} \end{cases} \qquad (7)$$

where $\vec{j}_s^{\omega}$ is the excitation current density in the coil and μ the permeability. Since $\vec{j}_s^{\omega}$ is in the azimuthal direction, the vector potential only has the azimuthal component. The influence of the arc on the magnetic field is two folds: the magnetic field produced by the arc current and that due to the eddy current induced within the arc. The magnetic field produced by the eddy current in the arc is negligible in comparison with that produced by the excitation current without the arc. Thus, the modification to the magnetic field due to the arc can be calculated by using equation (5). The total magnetic field is therefore the superposition of that produced by the coil without the arc and that due to the arc.

For moderately high currents, the arc can be treated as axisymmetrical and the current collection at the hollow cathode is through the introduction of a transparent electrode as in the case for auto-expansion breaker. The magnetic field produced by the excitation coil has radial and axial components, which interact with the radial and axial components of the current density to generate azimuthal movement of the arc. Thus, an azimuthal momentum equation is introduced to account for the azimuthal movement (Table 1).

2.2.2 *Computer simulated results*

Computer simulated results are given for the breaker (Figure 9), where the domain of computation for magnetic field is considerably larger than that for the electric field. A sinusoidal current of 50 Hz with a peak current of 10kA is used for the simulation for a given speed of contact separation of 3m/s. Typical temperature, pressure, electrical potential and velocity fields at the current peak are shown in Figure 10. The pressure rise in the expansion volume is mainly due to the compression of the gas by the arc and the thermal energy brought into the expansion volume by convection. The filling pressure is 2bar.

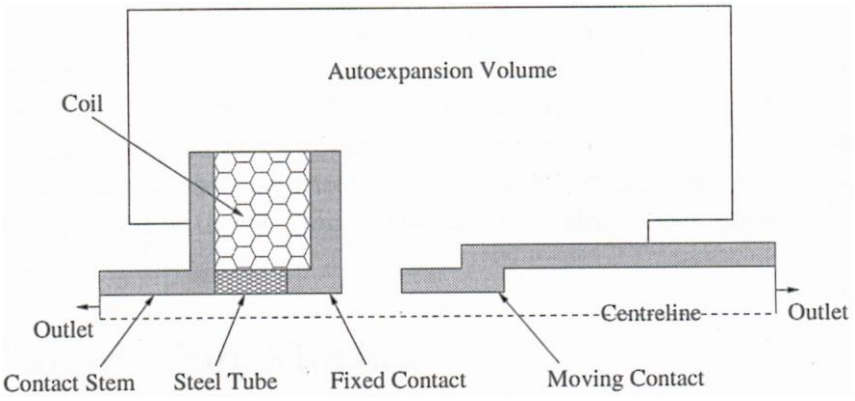

Figure 9 Schematic diagram of the LG interrupter.

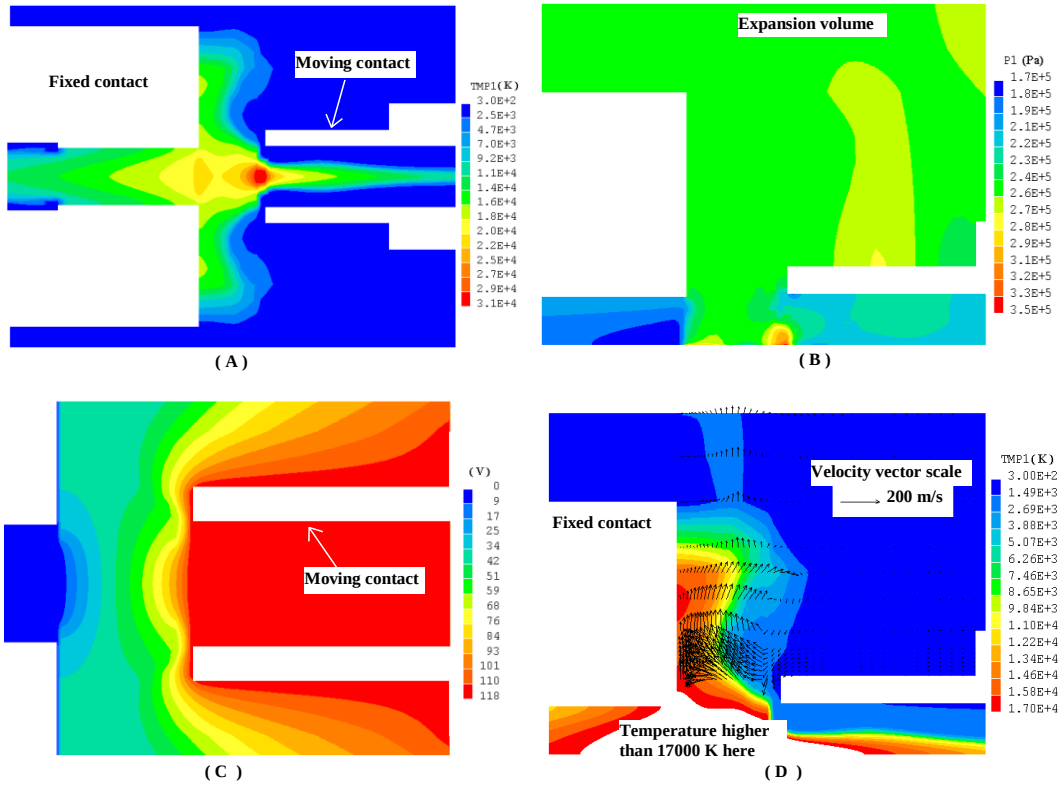

Figure 10 Distribution of temperature, pressure, electrostatic potential and velocity in LG circuit breaker at the peak current of 10kA. A) temperature, B) pressure, C) electrostatic potential and D) velocity.

The distinctive feature of the device is due to the Lorentz force associated with the magnetic field produced by the excitation coil. This force is a rotational force. The flow pattern is extremely complex due to the vortices, the centres of which are usually a low pressure region. Of the force components which generate arc rotation the

component associated with the radial current density and axial magnetic field component is dominant. Thus the direction of rotation will change if the direction of radial current density changes. This is clearly shown in Figure 11, where the arc consists of two "rotational" discs in the opposite direction, which is an extremely unstable situation. Turbulence in the presence of axisymmetric swirling can be very different from that of axisymmetric flow. Further investigation is needed in this respect.

When the arcing current is small, it is unlikely that the device can be treated as axisymmetrical. The arc rooting as well as arc instability make a three-dimensional modelling unavoidable. Because the arc rooting mechanism is not understood fully, it is not possible at present to include arc roots in the modelling.

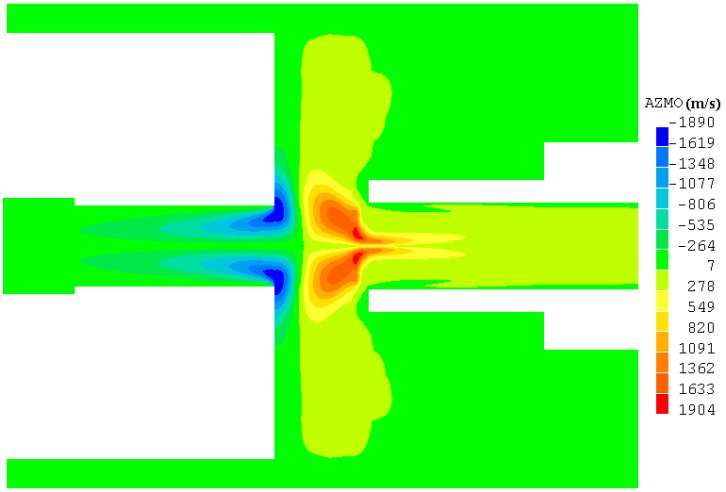

Figure 11 Distribution of the azimulthal velocity component in the LG breaker at the peak current of 10kA. Definition of the Lorentz force in the azimulthal direction is based on a LFS coordinate system.

3. Microwave Generated Plasma Jet

For material processing and light sources where impurities due to electrode melting must be avoided, electrodeless discharges have the definite advantages. Such a discharge can be produced using a microwave source (Figure 12),

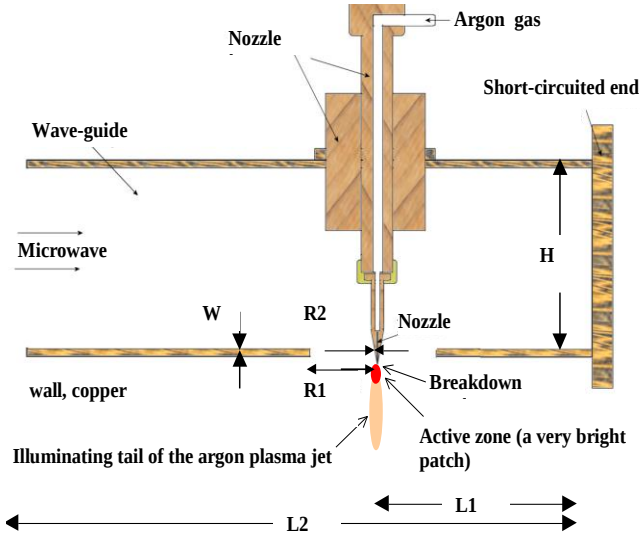

Figure 12 Schematic diagram of the wave-guide and nozzle geometry. The size of the plasma jet is only illustrative. Dimensions in mm: L1=115, L2=1012, H=129, W=2, R1=25, R2=0.6.

where the high electric field in the vicinity of the nozzle exit causes high frequency breakdown. A high velocity plasma jet is maintained by the self-focusing action of the microwave field. Spectroscopic measurements show

that the plasma in the active zone is not in local thermal equilibrium. For the atmospheric jet, collisions are sufficiently frequent to ensure electrons, argon ions and atoms move with the same velocity. However, since the energy transfer through elastic collisions is not efficient the electron temperature is therefore higher than that of heavy particles.

3.1 The governing equations

The flow in the axisymmetric plasma jet is described by the overall mass and momentum conservation equations as described by equation (1). The flow is assumed to be laminar. The conservation equation of translational energy for heavy particles is

$$\frac{\partial}{\partial t}(\frac{5}{2}\rho k_b T_h)+\nabla\cdot[\rho\vec{V}(\frac{5}{2}\rho k_b T_h)-\frac{k_{hl}}{c_{pa}}\nabla\left(\frac{5}{2}k_b T_h\right)]=\frac{2m_e}{m_h}\frac{3k_b}{2}(T_e-T_h)n_e\gamma_{eh} \tag{8}$$

where T_h is the heavy particles translational temperature, T_e electron temperature, k_b the Boltzmann constant, k_{hl} the heavy particles thermal conductivity, c_{pa} the specific heat capacity at constant pressure, m_e the mass of electron, m_a the mass of argon atom, n_e the electron number density, and γ_{eh} the momentum transfer collision frequency between electrons and heavy particles. This equation is solved by the PHOENICS solver.

The electron number density conservation equation is

$$\frac{\partial}{\partial t}(n_e)+\nabla\cdot\left[n_e\vec{V}+\vec{g}\right]=\gamma_1=\alpha n_a\left[S(T_e)-\frac{n_e^2}{n_a}\right] \tag{9}$$

where n_a is the atom number density, α the recombination coefficient [5,6] and $S(T_e)$ the ratio for chemical equilibrium[6].

The electron diffusion flux $\vec{g}$, is dominated by ambipolar diffusion due to density gradient. It can be written as:

$$\vec{g}=-\frac{(n_a+2n_e)^2 m_a}{\rho}D_A\nabla(\frac{n_e}{n_a+2n_e}) \tag{10}$$

where D_A is the ambipolar diffusion coefficient [7].

The energy conservation equation for electrons reads

$$\begin{aligned}&\frac{\partial}{\partial t}(\frac{5}{2}k_b n_e T_e)+\nabla\cdot[(\frac{5}{2}k_b n_e T_e)\vec{V}-k_{el}\nabla T_e+\frac{5}{2}k_b g T_e]\\&\quad=(1-\Theta)\mathrm{Re}\langle\sigma\rangle(\vec{E}\cdot\vec{E}^*)-\frac{2m_e}{m_h}\frac{3k_b}{2}(T_e-T_h)n_e\gamma_{eh}-\gamma_1 E_i\end{aligned} \tag{11}$$

where k_{el} is the electron thermal conductivity, σ is the complex electrical conductivity[6] and $\vec{E}$ the electric field component of the microwave. A proportion of the ohmic power input, Θ, is used for excitation of argon atoms and ions. $\Theta = 0.85$ in the present work.

The governing equations for the microwave generated plasma flow are closed by equation of state of the plasma gas which is given by

$$P=n_e k_b T_e+(n_i+n_a)k_b T_h \tag{12}$$

Maxwell's equations are required for the computation of electric field at microwave frequency. The coupling between the plasma and microwave fields is through ohmic heating and the plasma permittivity. The full Maxwell equations can be reduced to the following form in the present work

$$\nabla \times \nabla \times \vec{E} = \left(1 - \frac{w_p^2}{w^2 + \gamma_{eh}^2}\right) w^2 \mu_0 \varepsilon_0 \vec{E} - j\left(\frac{\gamma}{w}\frac{w_p^2}{w^2 + \gamma_{eh}^2}\right) w^2 \mu_0 \varepsilon_0 \vec{E} \tag{13}$$

where w_p is the electron plasma frequency, w the angular frequency of microwave field, ε_0 the permittivity of free space and μ_0 the permeability. Solution to equation (13) is obtained by solving 4 scalar variable equations, 2 for the radial component (real and imaginary parts) and 2 for the axial component of $\vec{E}$.

3.2 Additional Solvers

Two user-defined subroutine: SOLVNETE and SOLVELEC, both are called in Group 19 of the GROUND file, are used to solve the electron continuity equation and the electron energy equation (SOLVNETE), and the electric field equations (SOLVELEC). The velocity components, the present value of n_e and T_e, and all necessary material properties required in the subroutine SOLVNETE are passed from the GROUND file. Updated value of n_e and T_e are passed back to the GROUND file to update the solution of other governing equations. A similar procedure applies to the subroutine SOLVELEC.

3.3 Grids and other input functions

The grid system used in the simulation is shown in (Figure 13). The grid system used in the user-defined solvers is the same as that used by the PHOENICS solver. Solutions to the above equations are subjected to the appropriate boundary conditions for axisymmetric plasma jet (Figure 14). The radial velocity and the radial component of electric field and the radial derivatives of all other relevant quantities should vanish on the axis. The axial and radial derivatives of all quantities are set zero far away from the plasma jet.

The argon gas flows into the domain with a velocity profile given by

$$w = w_{in}^{\max}\left(1 - \left(\frac{r}{R_{OA}}\right)^2\right) \tag{14}$$

where $w_{in}^{\max}$ is adjusted to give the required flow rate and R_{OA} is the radius of the nozzle hole.

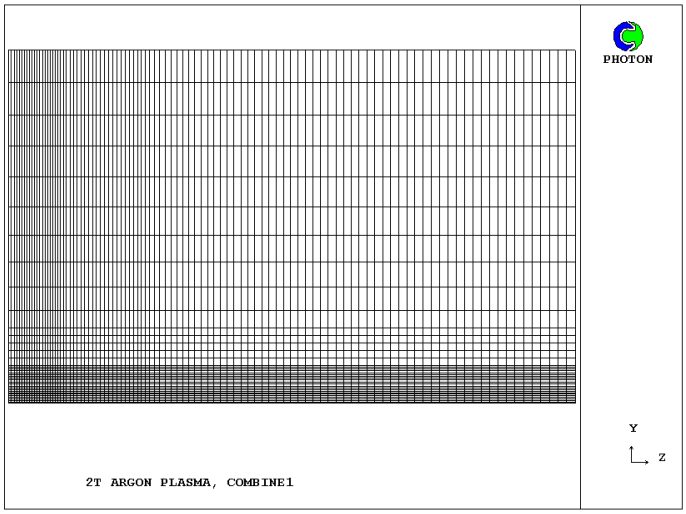

Figure 13 Schematic diagram showing grid used for simulation.

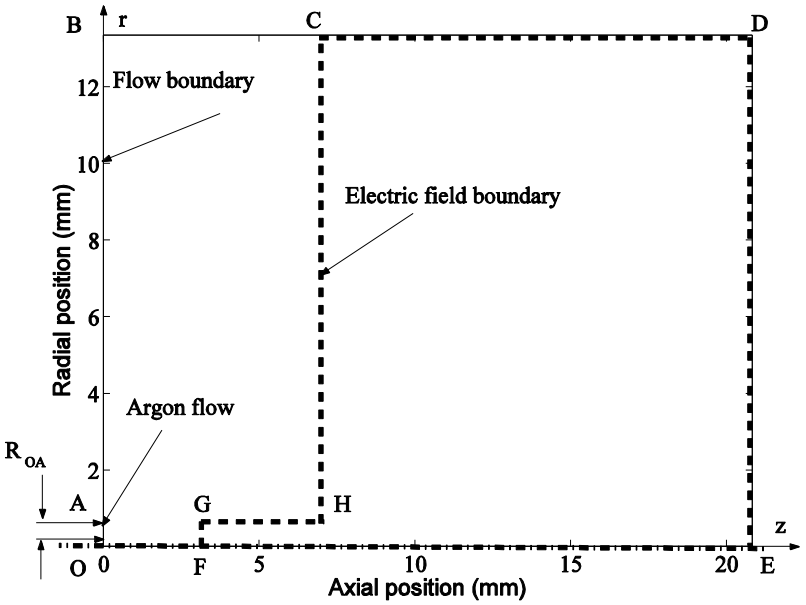

Figure 14 Schematic diagram showing the boundary conditions used for simulation. The exit of the nozzle is located at z=0mm.

The boundary conditions for the real part of the axial electric field need special consideration. The discharge is first initiated in a small region close to the nozzle exit. The rapid increase in the electron number density in this region affects the field distribution. The increased electrical conductivity tends to guide the microwave along the surface of this active region.

A steady state is reached when the electric field along the surface of this active zone is just sufficient to maintain the energy balance and the balance between ionisation and charge loss mechanisms. The field along FGHCDEF (Figure 14) is specified. With the specified field conditions the governing equations are solved simultaneously.

3.4 Computational results

Attention is focused on the case for which the power from the source generator is 3kW and the argon flow rate of 5l/min. Electron temperature and number density are important plasma parameters affecting the ionisation state, the complex electric conductivity of the plasma, and the energy transfer to heavy particles. The contours of electron and heavy particles temperature are shown in Figures 15 and 16 respectively, while the radial profiles of electron number density at three axial stations are plotted in Figure 17, where experimental results are also given.

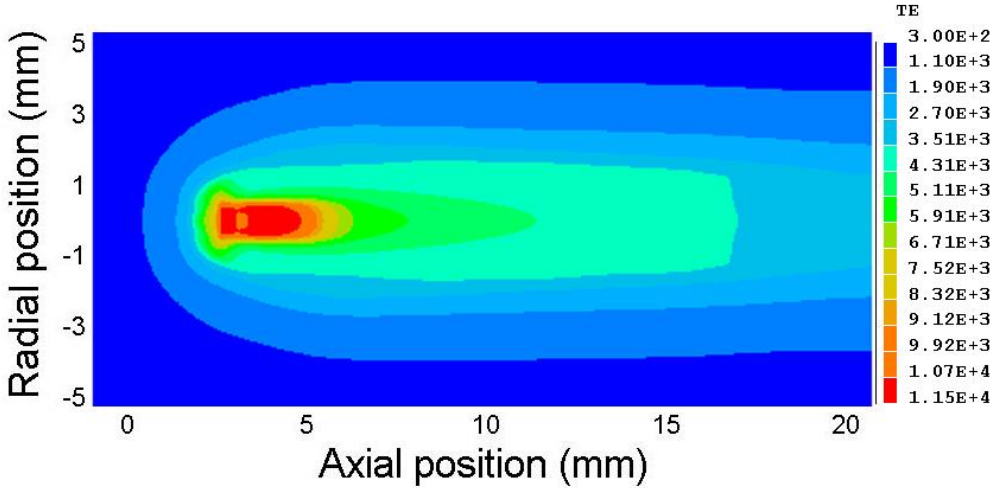

Figure 15 Electron temperature distribution at 3kW microwave source power and 5l/min Argon flow rate.

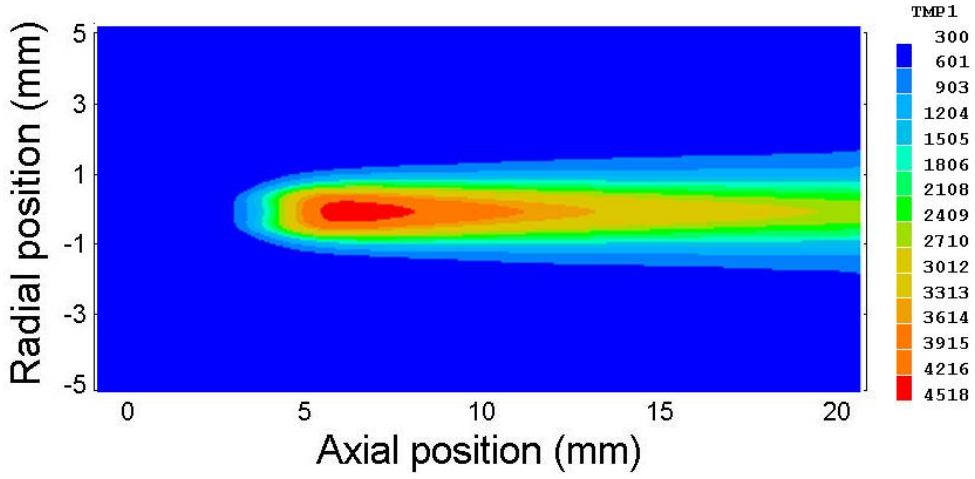

Figure 16 Heavy particles translational temperature distribution at 3kW microwave source power and 5l/min Argon flow rate.

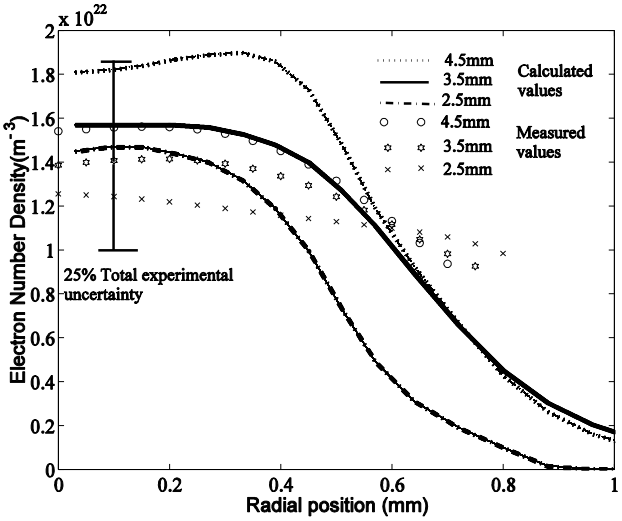

Figure 17 The radial profiles of electron number density at three axial stations (2.5mm, 3.5mm and 4.5mm), together with experimental results from [8]. Total experimental uncertainty is 25%. Error bar shown is for the case located at 3.5mm.

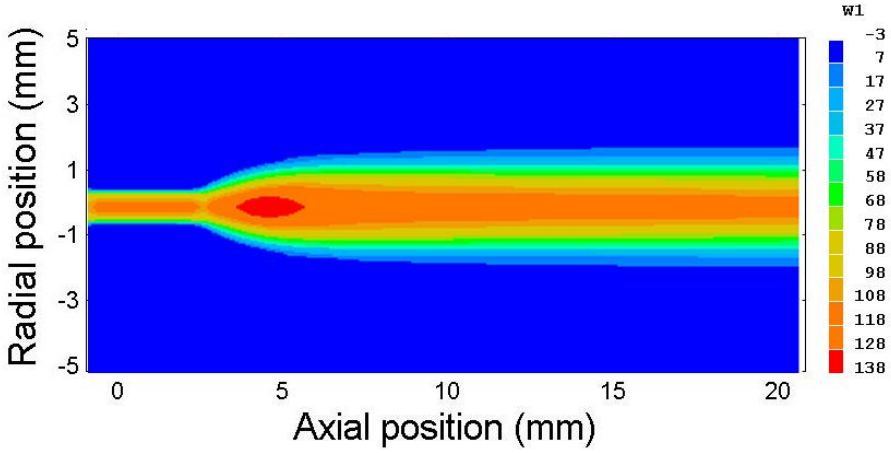

Figure 18 Axial velocity of the plasma jet at 3kW microwave source power and 5l/min Argon flow rate.

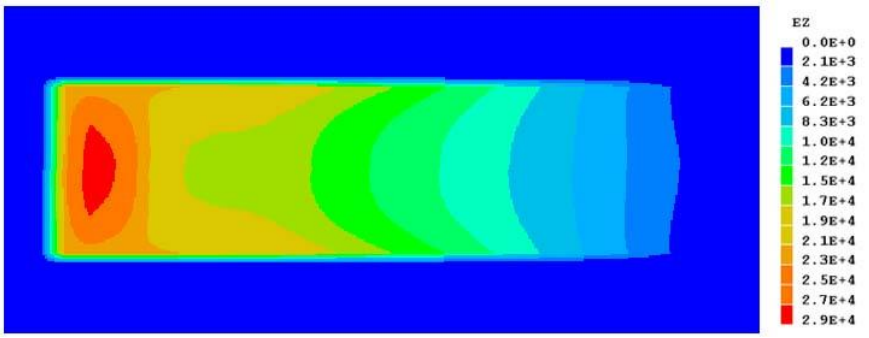

Figure 19 Axial electric field distribution at 3kW microwave source power and 5l/min Argon flow rate.

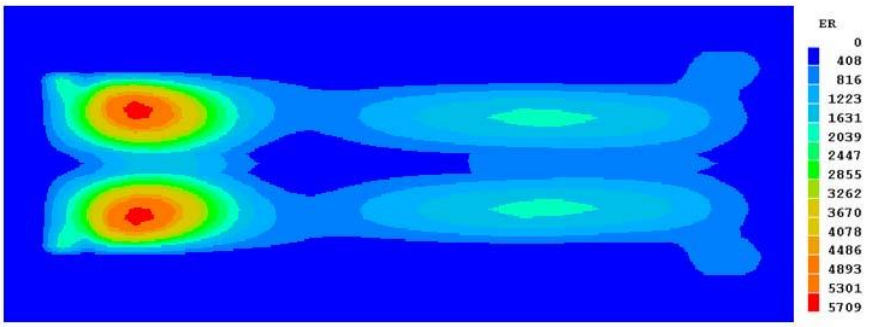

Figure 20 Radial electric field distribution at 3kW microwave source power and 5l/min Argon flow rate.

The axial velocity is shown in Figure 18. The maximum plasma velocity is 138m/s, and the maximum increase in pressure is around 3% above atmospheric pressure. The magnitude of the axial and radial electric field components are shown in Figures 19 and Figure 20 respectively.

The computed power input to the plasma jet is equal to 623W, which is approximately equal to 300W/mm^3 in the active zone. The overall energy balance of the plasma jet requires that the total enthalpy flux reaching a work piece is equal to the power input into the active zone.

4. Conclusions

It has been demonstrated that with a modern PC the complex physical processes occurring in circuit breaker arcs and microwave-generated atmospheric plasma can be simulated using PHOENICS. Modelling of arc flow surrounding a moving contact has been successfully implemented and the results are verified. Flow fields, temperature, pressure, electric and magnetic fields can be visualised in detail. The effects of changing one design parameter can be clearly shown and its influence on breaker performance easily assessed. Additional solvers in terms of user-defined subroutines have been linked to a recompilable version of PHOENICS through an interface in GROUND to obtain solutions for the electric field at microwave frequency, electron number density and electron temperature, whose governing equations cannot be solved by PHOENICS solvers. This extended the application of PHOENICS to modelling a two-temperature non-LTE plasma. It is therefore concluded that computer simulation based on PHOENICS can be used as a powerful design aid, especially for technological plasma systems with axisymmetric flow.

Acknowledgement

The authors thank VA Tech Reyrolle, LEE Foundation of Singapore and Malaysia, LG Industrial Systems Ltd in Cheong Ju, Korea and the EPSRC of the UK for financial support during the course of development of computer simulation tools. Dr A B Murphy of CSIRO, Sydney, Australia has provided the thermodynamic and transport data for PTFE/SF_6 mixtures.

References

[1] J L Zhang, J D Yan, A B Murphy, W Hall and M T C Fang, "Computational Investigation of Arc Behaviour in an Auto-Expansion Circuit Breaker Contaminated by Ablated Nozzle Vapour", to be published in IEEE Transactions on Plasma Science, 2002.

[2] D G Lilley, "Prediction of Inert Turbulent Swirl Flows", AIAA Journal, vol. 11, pp. 950-960, 1973.

[3] A B Murphy, Private communication.

[4] J D Yan, M T C Fang and W Hall, "The Development of PC based CAD Tools for Auto-expansion Circuit Breaker Design", IEEE Trans. on Power Delivery, Vol.14, pp.176-181, 1999.

[5] M I Hoffert and H Lien, "Quasi-one-dimension, nonequilibrium gas dynamics of partially ionized two-temperature argon", Phys. Fluids 10, pp1769, 1967.

[6] M Mitchner and C H Kruger, "Partially ionized gases", John Wiley and Sons, New York, 1973.

[7] R S Devoto, "Transport coefficients of partially ionized argon", Phys. Fluids 10, pp354, 1967.

[8] J D Yan, C F Pau, S R Wylie and M T C Fang, "Experimental characterisation of an atmospheric argon plasma jet generated by an 896MHz microwave system", on press, 2002.